

Electronic Supporting Information (ESI)

A tetra-nuclear Cu(II) complex of amide-imine conjugate: highly selective ESIPT based probe for OCl⁻

Jayanta Das^a, Sabyasachi Ta^a and Debasis Das^{a*}

^aDepartment of Chemistry, The University of Burdwan, Burdwan, 713104, W.B., India
E-mail: ddas100in@yahoo.com (D. Das)

1. Materials

High purity HEPES buffer, 2-hydroxy-benzoic acid, 3-ethoxy-2-hydroxy-benzaldehyde, hydrazine (NH_2NH_2), sodium hypochlorite (NaOCl) and thionyl chloride (SOCl_2) are purchased from SigmaAldrich (India). Reagent grade $\text{Cu}(\text{NO}_3)_2 \cdot 6\text{H}_2\text{O}$ have been purchased from Merck (India). Spectroscopic grade solvents have been used. Other chemicals are of analytical reagent grade. Mili-Q Milipore ($18.2 \text{ M}\Omega \text{ cm}^{-1}$) water is employed as and when required.

2. Physical measurements

The PerkinElmer 2400 series II CHN analyzer is used to perform elemental analysis. FTIR spectra are captured with Shimadzu IR spectrometer (model IR Prestige 21 CE). Shimadzu Multi Spec 2450 spectrophotometer and Hitachi F-7000 spectro-fluorimeter are used for collection of absorption and emission spectroscopic data.

The pH is measured with Systronics digital pH meter (model 335) where HCl/NaOH (50 μM) is used for adjustment of pH. Electrospray ionization mass spectra (ESI-mass) are recorded using Fisher Thermo scientific Exactive Mass Spectrometer (positive or negative mode). MALDI-TOF mass spectra are recorded using Bruker UltraFlextreme mass spectrometer. $^1\text{HNMR}$ and $^{13}\text{CNMR}$ spectra are recorded using Bruker 400 MHz spectrometer using $\text{DMSO}-d_6$ as solvent. The chemical shift values are presented in ppm while residual solvent peak is used as internal reference. Multiplicity is indicated as follows: s (singlet), d (doublet), t (triplet), q (quartet), m (multiplet). Coupling constants (J , s) are reported in Hertz (Hz). Time-resolved fluorescence lifetime measurements are performed with FluoroCube-01-NL spectrometer using Laser-diode (Model: DD-450L-8666, typical FWHM ~ 170 ps, $\lambda_{\text{ex}} = 336$ nm).

Single crystal X-ray data are collected on a Bruker X8 APEX-II CCD diffractometer at 100(2) K using graphite-monochromated Mo-K α radiation (0.71073\AA) at 150K. Data are processed and corrected for Lorentz and polarization absorption effects. Crystal structure is

solved by standard direct methods using the SHELXS¹ and refined by full-matrix least-squares with SHELXL,² and OLEX2 software.³ Significant crystal parameters and refinement data are presented in **Table S1 (ESI)**. All non-hydrogen atoms are refined with anisotropic thermal displacements. Hydrogen atoms are included in the structure factor calculation in geometrically idealized positions, with thermal parameters depending on the parent atom, using a riding model. Images are generated by Mercury software.⁴

3. General method of UV-Vis and fluorescence titration

The cuvettes used for measurement of absorption and emission spectra are of 1cm path length. A 20 μM stock solution of **C1** is prepared in EtOH/ H₂O media (1/1, v/v) for absorption and emission spectroscopic studies. Stock solution of sodium hypochlorite (5%, wt./ volume) is prepared with deionized water. The working solutions of **C1** and **OCl⁻** are then prepared from respective stock solutions with appropriate dilution. Fluorescence data are collected using 5 nm × 5 nm slit width.

4. Job's plot from fluorescence experiment

A series of solutions containing **C1** and **OCl⁻** are prepared in such a way that the total concentration of **OCl⁻** and **C1** remain constant (20 μM) in all the sets. The mole fraction (**x**) of **OCl⁻** is varied from 0.05 to 0.9. The emission intensity of [C1-OCl] adduct at 483 nm is plotted against the mole fraction of **C1**.

5. Calculation of quantum yield

Following equation⁵⁻⁶ is used to calculate fluorescence quantum yield of the species relative to anthracene whose quantum yield is known (**Φ =0.27**) in ethanol medium.

$$\Phi_s = \Phi_r \frac{A_r F_s \eta_s^2}{A_s F_r \eta_r^2}$$

Where A_s and A_r are the absorbance of the sample and reference solutions respectively, at the same excitation wavelength, F_s and F_r are corresponding relative integrated emission intensities and η is the refractive index of the solvent.

6. Determination of binding constant

The binding constant of **C1** for **OCl⁻** is determined using Benesi-Hildebrand equation⁷, written below

$$\frac{F_{max} - F_{min}}{F_X - F_{min}} = 1 + \frac{1}{K[C]^n}$$

Where F_{\min} , F_x , and F_{\max} are the emission intensities of the C1 in absence of OCl^- , at an intermediate OCl^- concentration, and at a concentration of complete interaction with OCl^- respectively. K is the binding constant, C is the concentration of OCl^- and n is the number of OCl^- bound per probe molecule (here, $n = 4$). The value of K is obtained from the slope of the plot.

7. Calculation of detection limit

The detection limit (**DL**) is determined from the following equation⁸

$$DL = \frac{3\sigma}{S}$$

σ is the standard deviation of the blank solution, S is the slope of the calibration curve.

For determination of standard deviation, the emission intensities are measured 10 times.⁹

8. Time resolved emission spectra measurement

Fluorescence lifetime of C1-OCl⁻ adduct is measured using time correlated single photon counting (TCSPC) technique. The sample is excited using a picosecond diode laser and the fluorescence signal is recorded keeping the emission polariser at the magic angle (54.70) with respect to the excitation polariser to eliminate the loss of signal for the contribution of anisotropy decay and fluorescence decays were deconvoluted using DAS6 software.¹⁰ The relative contributions (α_n) to the fluorescence decay of the multi-exponential decay are obtained using the following relation^{11,12}

$$\alpha_n = \frac{B_n}{\sum_{i=1}^n B_i}$$

B_i is the pre-exponential factor of a single exponential decay. The average lifetime of the compound is calculated using the following relation:

$$\langle \tau \rangle = \frac{\sum_{i=1}^n \alpha_i t_i^2}{\sum_{i=1}^n \alpha_i t_i}$$

Reference

1. M. C. Burla, R. Caliandro, M. Camalli, B. Carrozzini, G. L. Casciaro, L. De Caro, C. Giacovazzo, G. Polidori and R. Spagna, *J. Appl. Crystallogr.*, 2005, **38**, 381-388.

2. G. M. Sheldrick, *Acta Cryst.*, 2008, **E64**, 112-122.
3. G. M. Sheldrick, *Acta Cryst.*, 2015, **A71**, 3-8.
4. O. V. Dolomanov, L. J. Bourhis, R. J. Gildea, J. A. K. Howard and H. Puschmann, *J. Appl. Cryst.*, 2009, **42**, 339-341.

5. W. H. Melhuish, *J. Phys. Chem.*, 1961, **65**, 229-235.
6. A. T. R. Williams, S. A. Winfield and J. N. Miller, *Analyst*, 1983, **108**, 1067-1071.
7. H. A. Benesi and J. H. Hildebrand, *J. Am. Chem. Soc.*, 1949, **71**, 2703-2707.
8. M. Zhu, M. Yuan, X. Liu, J. Xu, J. Lv, C. Huang, H. Liu, Y. Li, S. Wang and D. Zhu, *Org. Lett.*, 2008, **10**, 1481-1484.
9. S. Dey, R. Purkait, K. Pal, K. Jana, C. Sinha, *ACS Omega*, 2019, **4**, 8451-8464.
10. J. R. Lakowicz, Plenum, New York.
11. S. Banthia and A. Samanta, *J. Phys. Chem. B*, 2006, **110**, 6437–6440.
12. B. Ramachandram, G. Saroja, B. Sankaran and A. Samanta, *J. Phys. Chem. B*, 2000, **104**, 11824–11832.

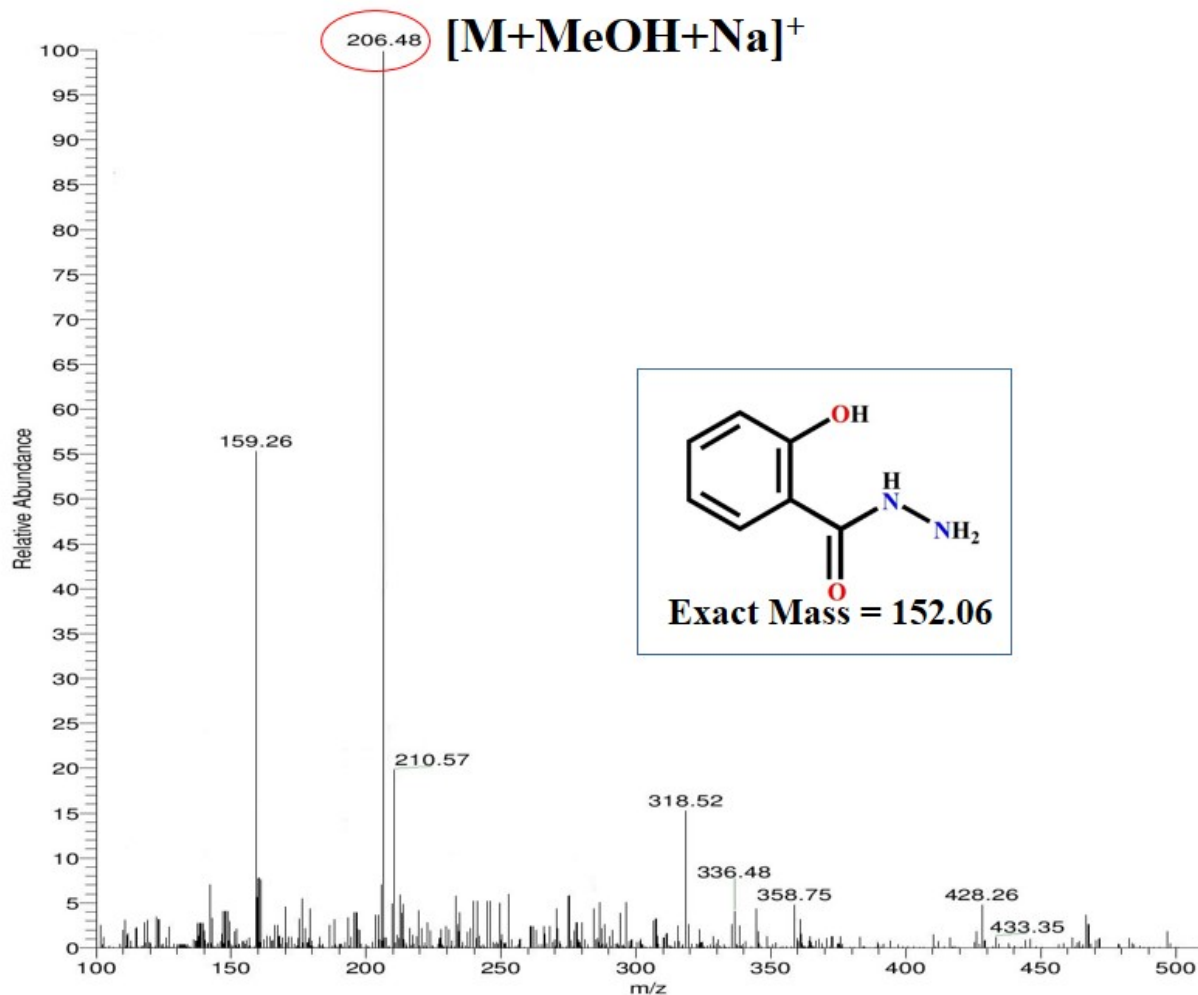


Figure S1a QTOF mass spectrum of **2HBA**.

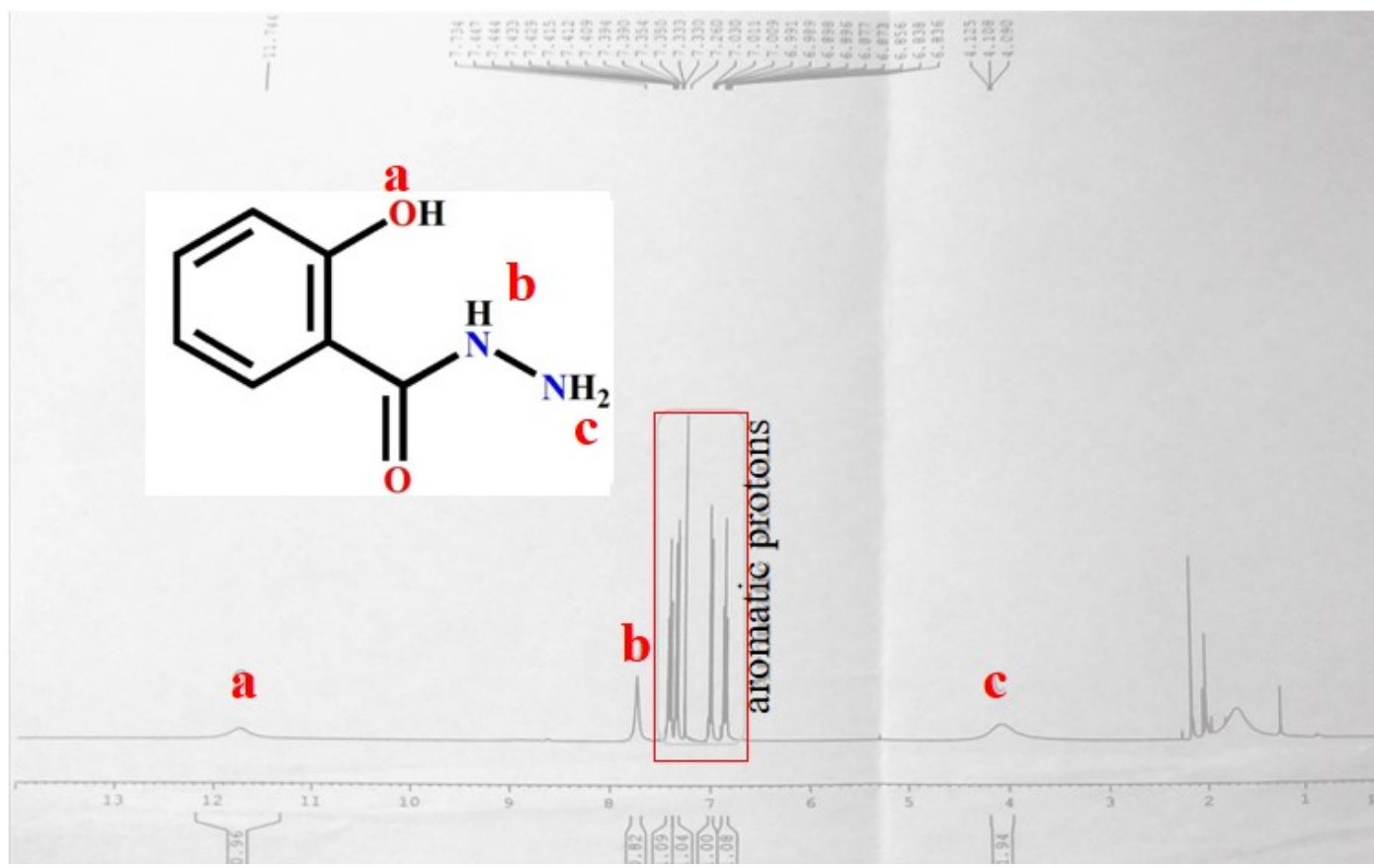


Figure S1b ^1H NMR spectrum of **2HBA**

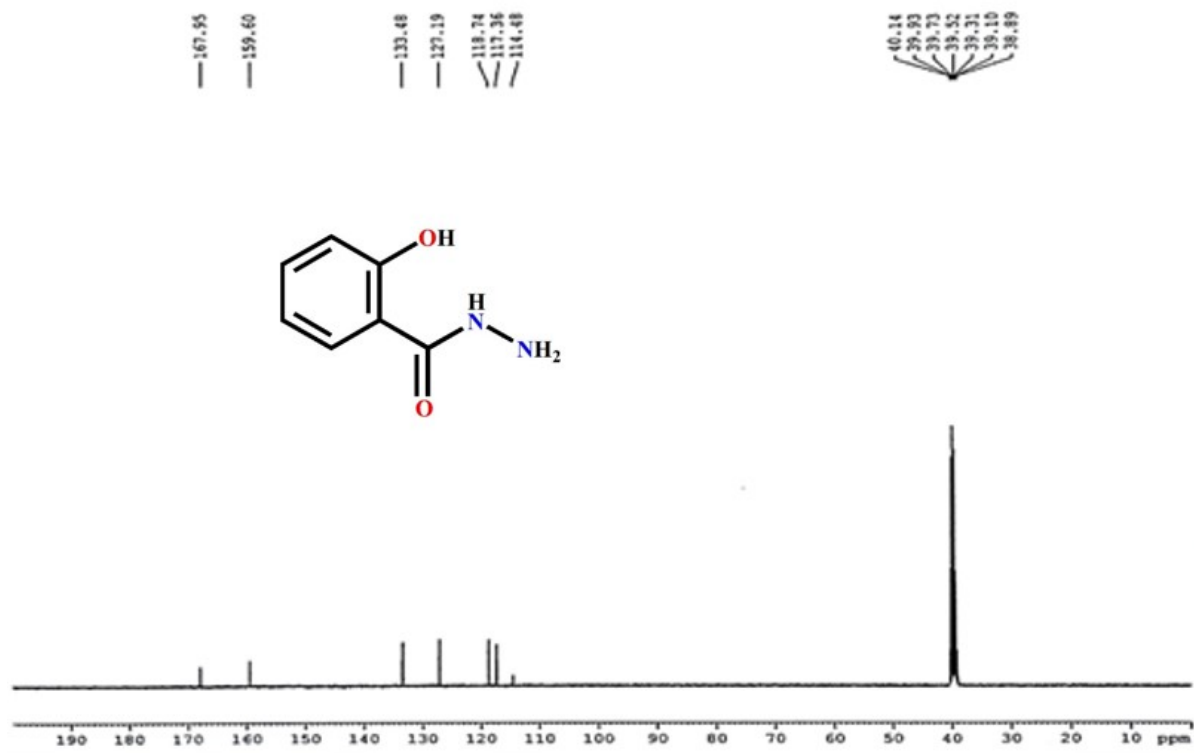


Figure S1c ^{13}C NMR spectrum of **2HBA**.

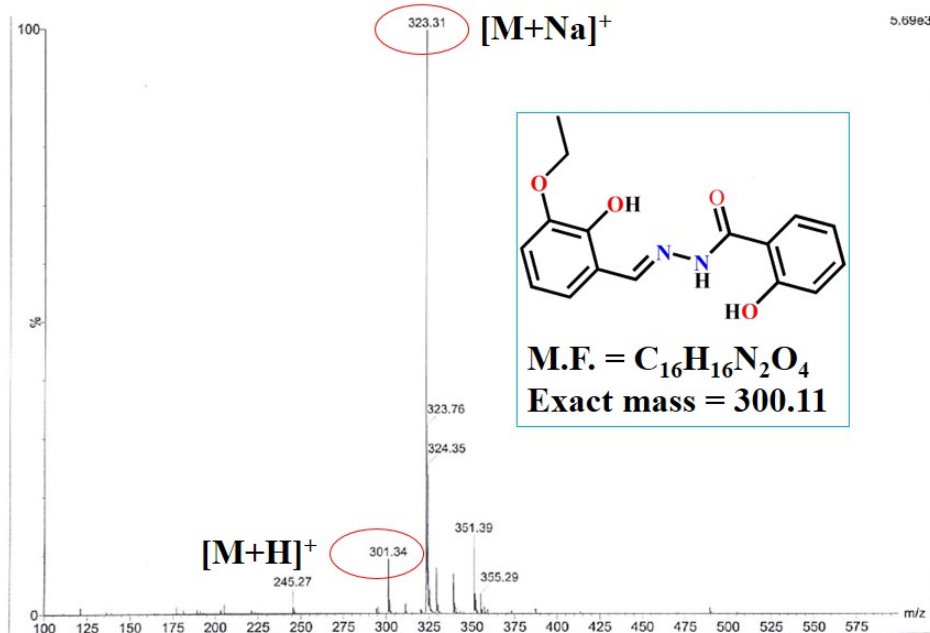


Figure S2a QTOF mass spectrum of H_2L .

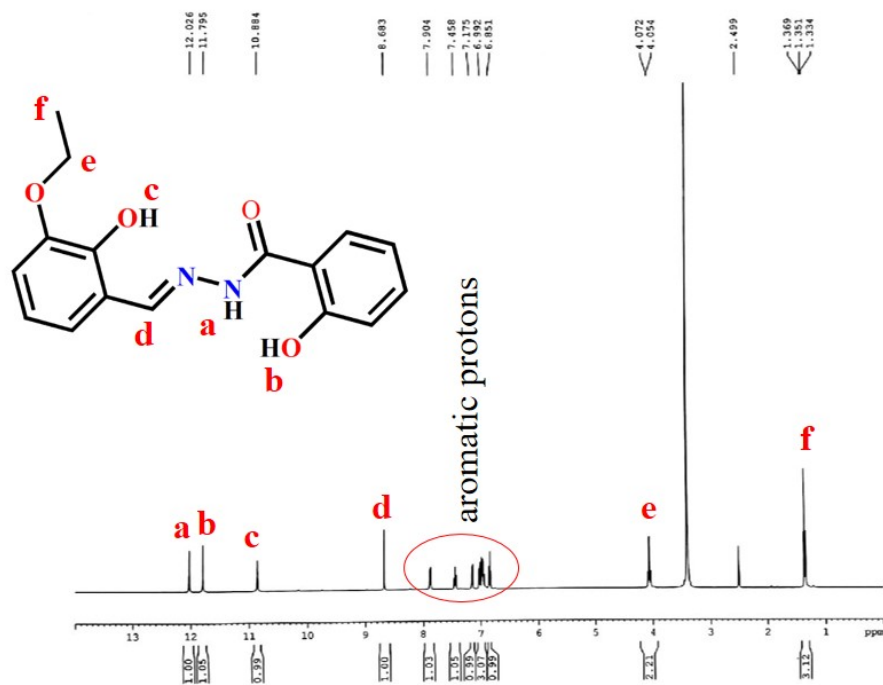


Figure S2b ^1H NMR spectrum of H_2L in DMSO-d_6

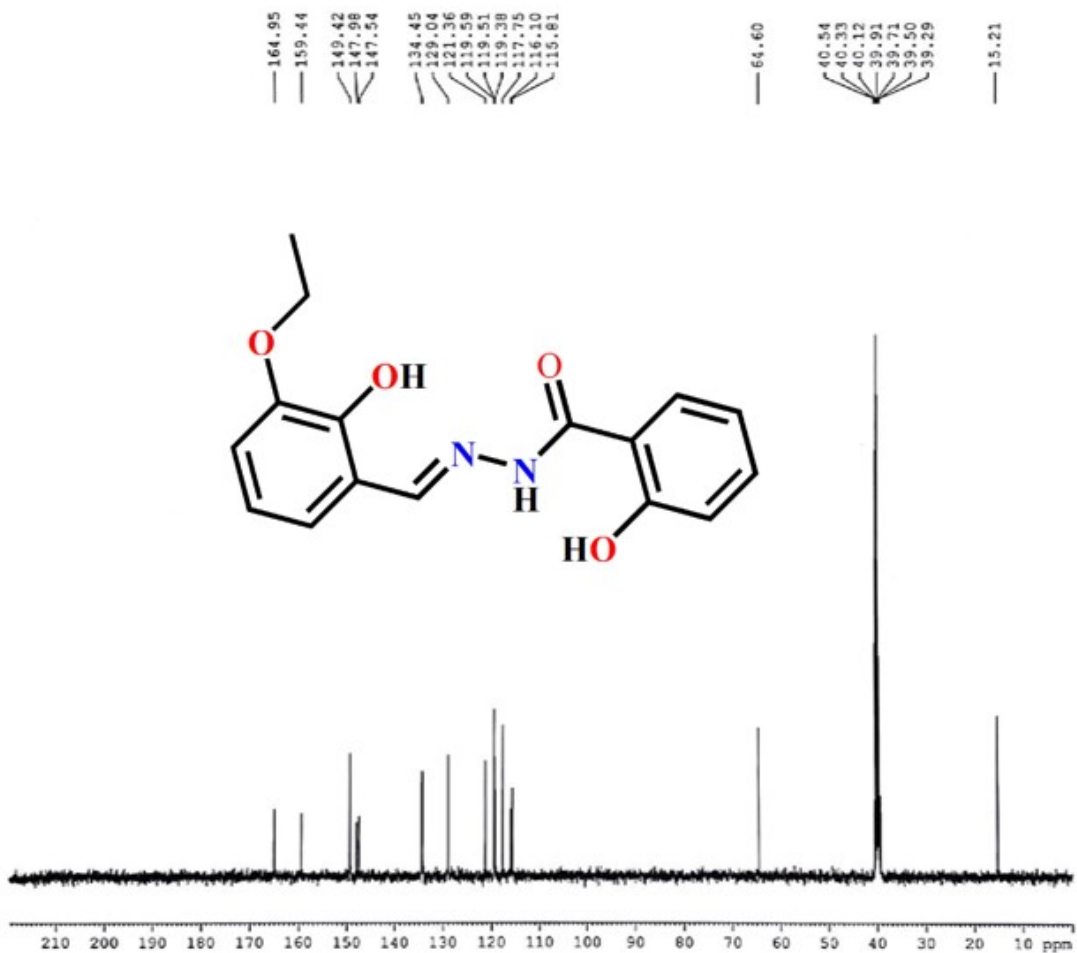


Figure S2c ^{13}C NMR spectrum of H_2L .

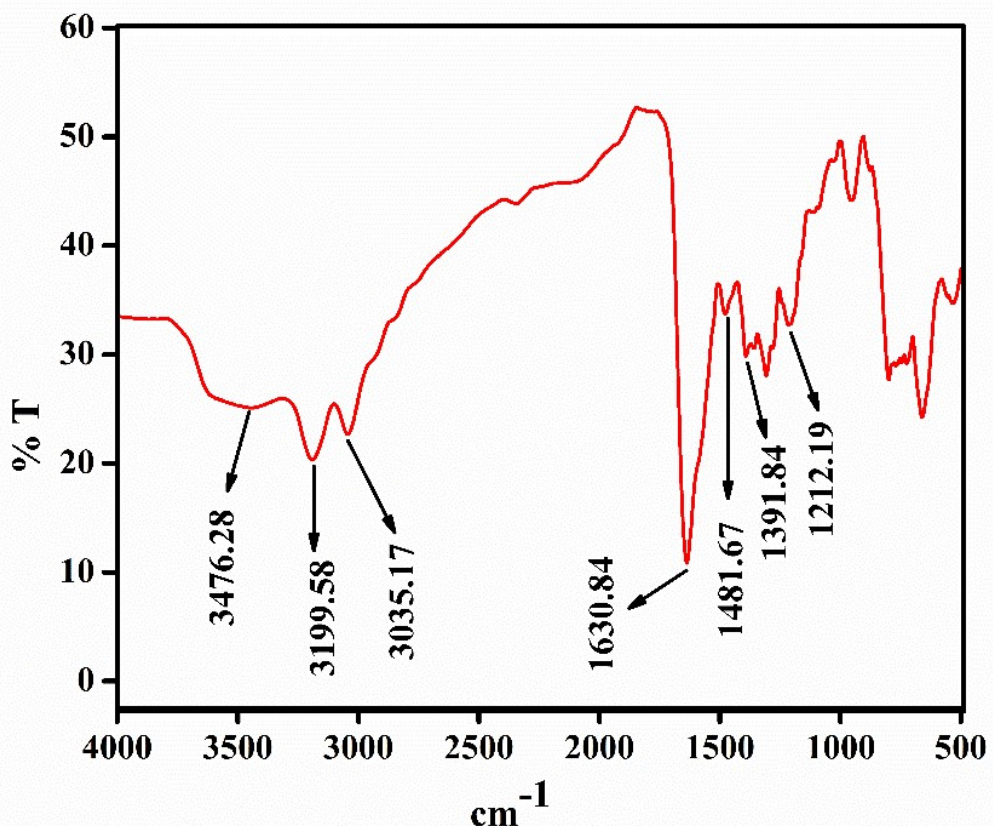


Figure S2d FTIR spectrum of H_2L

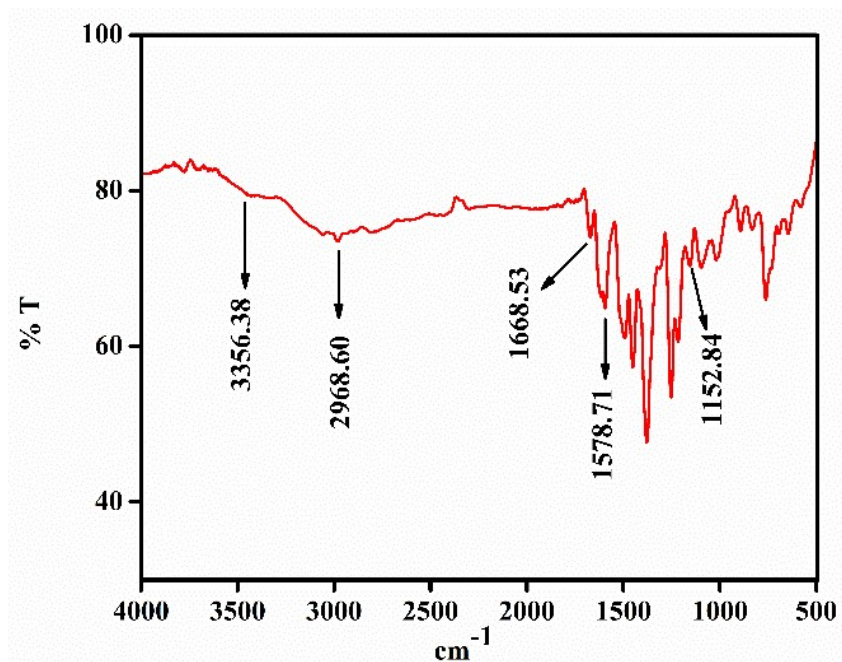


Figure S3a FTIR spectrum of compound C1

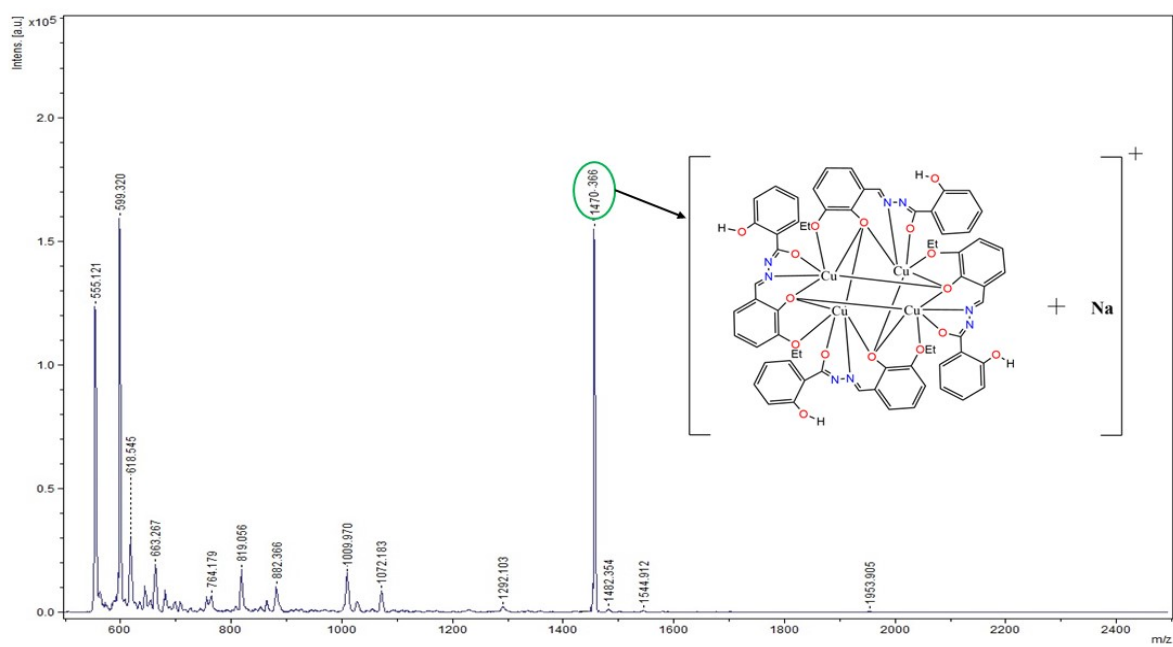


Figure S3b MALDI-TOF mass spectrum of **C1**

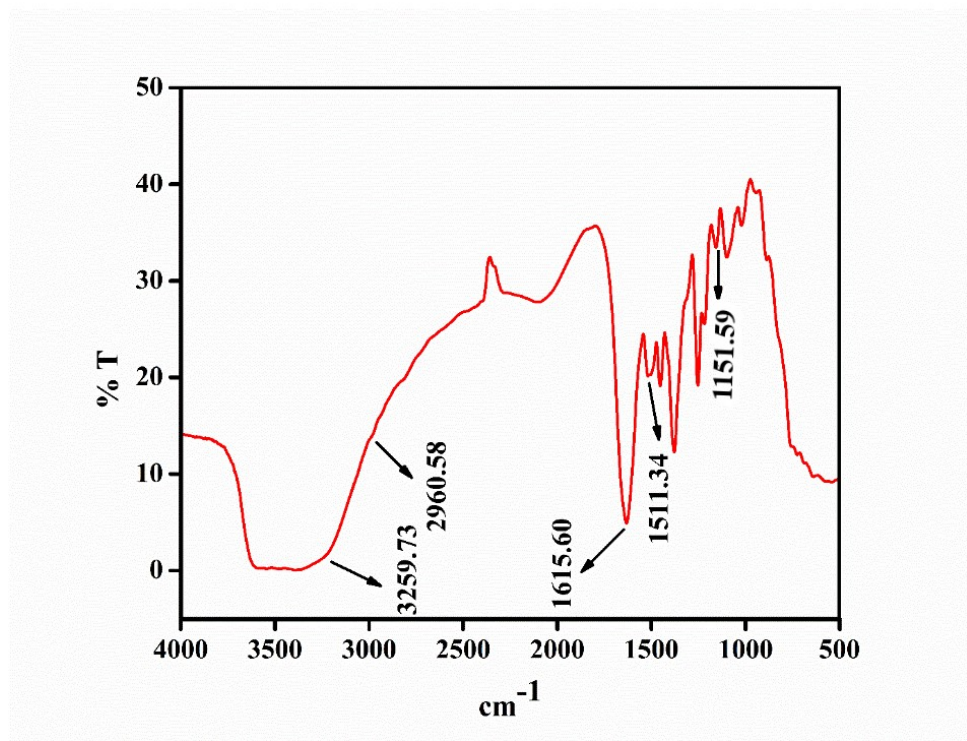


Figure S3c FTIR spectrum of $[\text{C1-OCl}^-]$ adduct

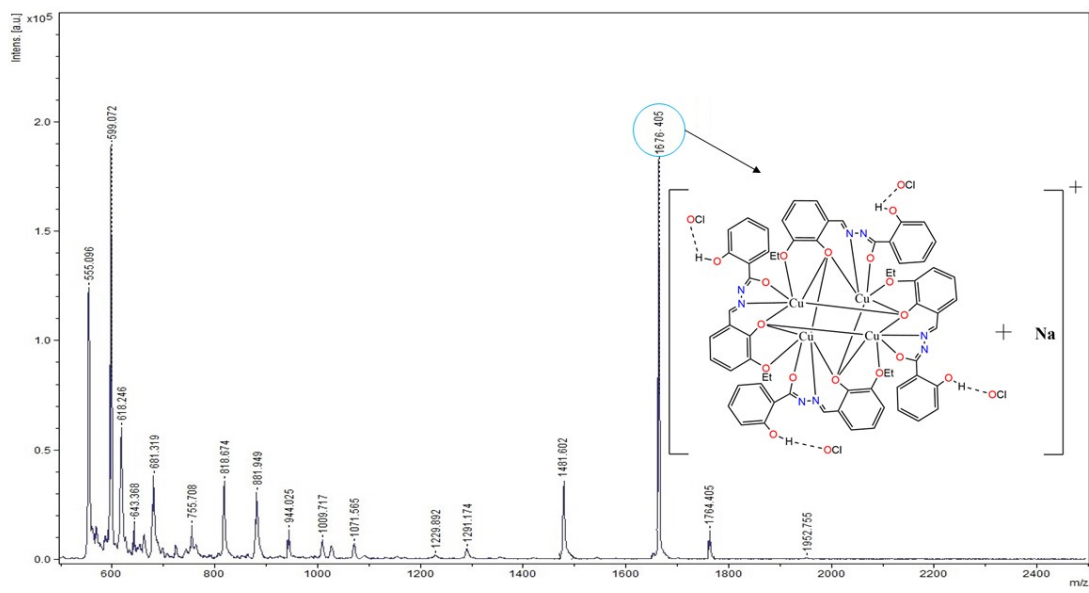


Figure S3d MALDI-TOF mass spectrum of [C1-OCl] adduct.

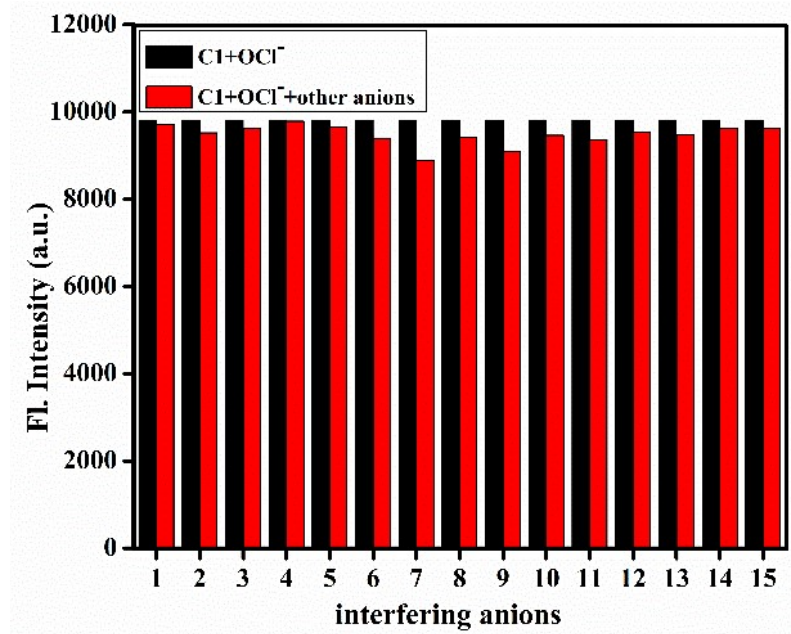


Figure S4 Interference of other anions during determination of OCl^- using **C1** by fluorescence method ($\lambda_{\text{ex}} = 352 \text{ nm}$, $\lambda_{\text{em}} = 483 \text{ nm}$); 1 = F^- , 2 = Cl^- , 3 = Br^- , 4 = I^- , 5 = NO_3^- , 6 = NO_2^- , 7 = SO_4^{2-} , 8 = AsO_2^- , 9 = AsO_4^{3-} , 10 = SCN^- , 11 = ClO_4^- , 12 = HSO_4^- , 13 = H_2PO_4^- , 14 = N_3^- , and 15 = AcO^- .

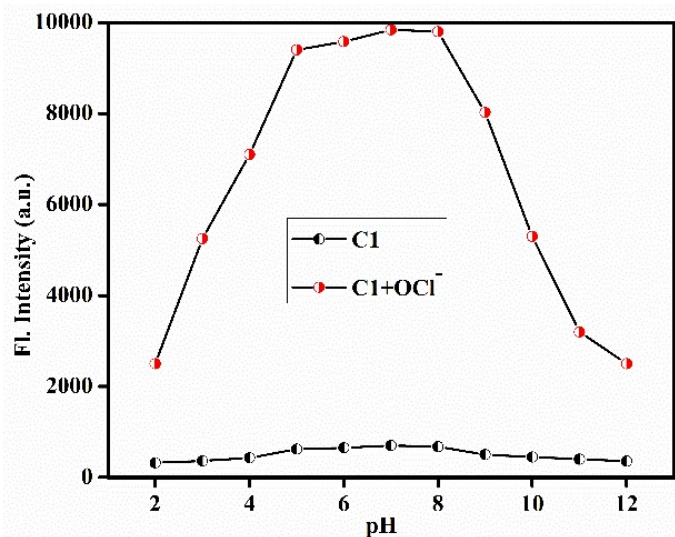


Figure S5 Effect of pH on the emission intensities of **C1** ($\lambda_{\text{ex}} = 352 \text{ nm}$ $\lambda_{\text{em}} = 483 \text{ nm}$) in presence and absence of **OCl⁻**.

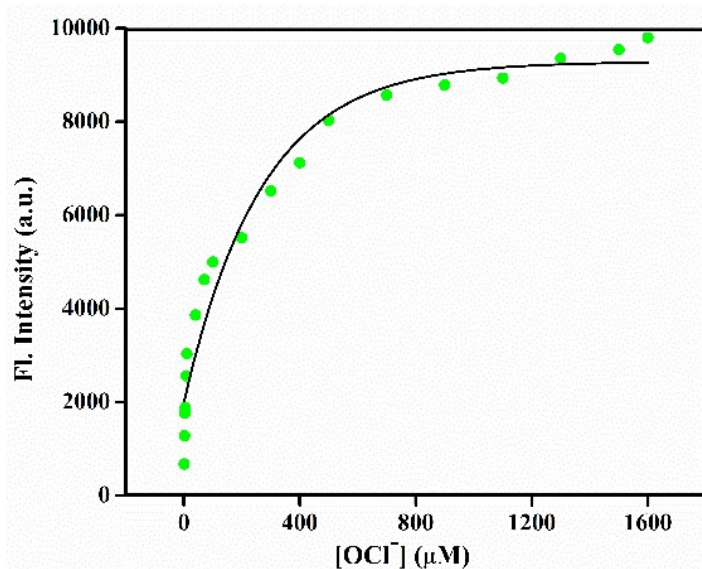


Figure S6 Plot of emission intensities of **C1** (20 μM , $\lambda_{\text{ex}} = 352 \text{ nm}$, $\lambda_{\text{em}} = 483 \text{ nm}$) as a function of externally added **OCl⁻** (1.0-1600 μM).

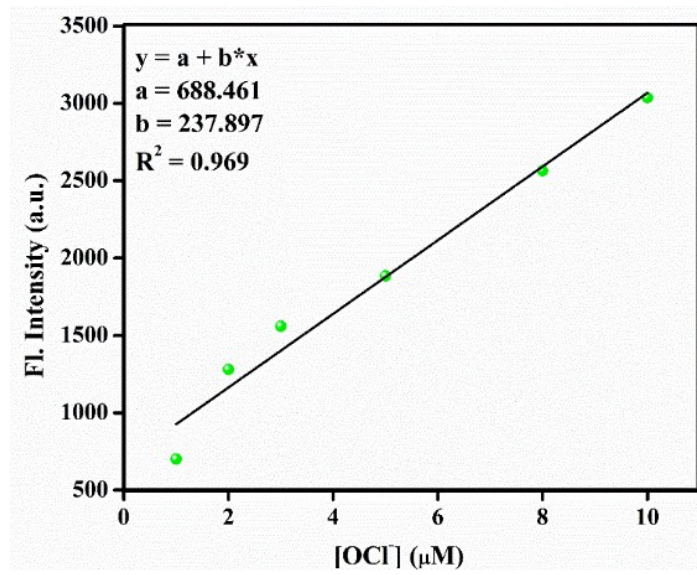


Figure S7 Determination of detection limit based on change in the ratio (fluorescence intensity at $\lambda_{ex} = 352$ nm, $\lambda_{em} = 483$ nm) of **C1** (20 μM) with **OCl** (linear portion of **Figure S6**)

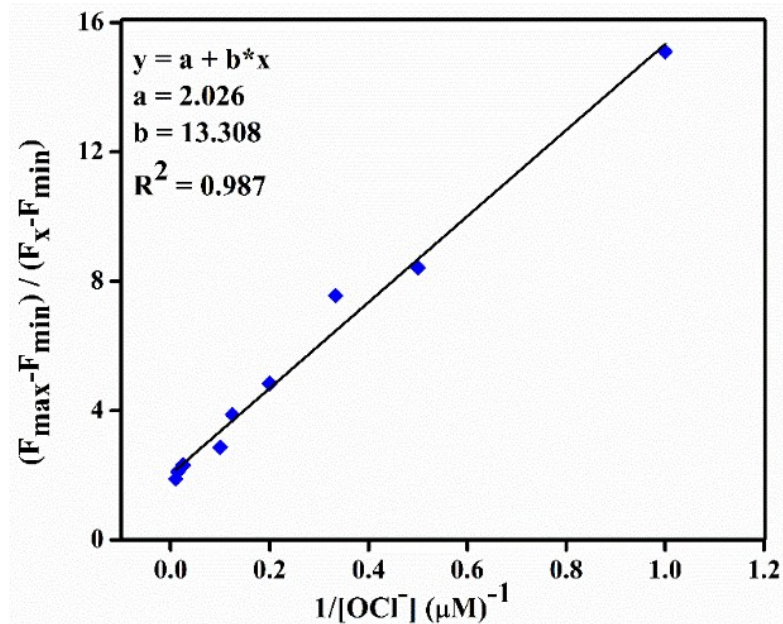


Figure S8 Benesi–Hildebrand plot for determination of association constant of **C1** with **OCl** (linear portion only), $\lambda_{ex} = 352$ nm, $\lambda_{em} = 483$ nm.

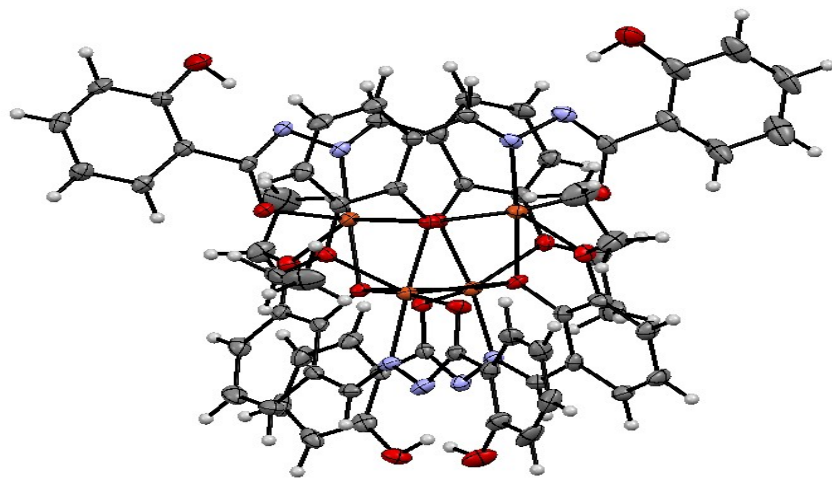


Figure S9 ESIPT active (ORTEP) view of C1

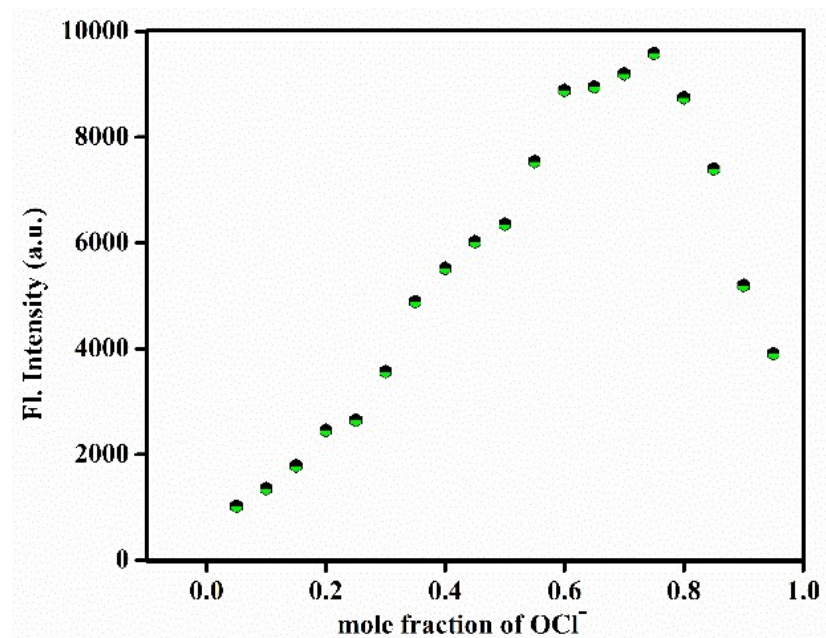


Figure S10 Job's plot for determination of stoichiometry of $[\text{C1- OCl}^-]$ adduct ($\lambda_{\text{ex}} = 352$ nm, $\lambda_{\text{em}} = 483$ nm.).

Table S1 Crystal data and structure refinement for C1

Complex	C1
CCDC	1830263
Empirical formula	$\text{C}_{64}\text{H}_{56}\text{Cu}_4\text{N}_8\text{O}_{16}$
Formula weight	1447.37
Crystal system	Trigonal
Space group	R 3 c
Hall group	R 3 -2" ^c

Temparature	150 K
Wavelength	0.71073
<i>a</i> /Å	27.520(4)
<i>b</i> /Å	27.520(4)
<i>c</i> /Å	43.305(7)
$\alpha/^\circ$	90
$\beta/^\circ$	90
$\gamma/^\circ$	120
Volume/Å ³	28403(9)
<i>Z</i>	18
ρ_{calc} g/cm ³	1.523
μ/mm^{-1}	1.405
F(000)	13320
F(000')	13348.18
Θ_{max}	25.458
Index ranges (<i>h,k,l</i> max)	33,33,52
Reflections collected	0.0402(8421)
wR ₂ (Reflection)	0.0975(11175)
S	1.102
Npar	845
Data completeness	2.00/1.00

Table S2 Selected bond lengths [Å] and angles [°] for C1

ATOMS	LENGTH	ATOMS	ANGLE
Cu1 O2A	1.932(5)	O2A Cu1 O3A	172.6(2)
Cu1 O3A	1.960(5)	O2A Cu1 O3B	96.91(19)
Cu1 N2A	1.910(6)	O2A Cu1 O3C	96.6(2)
Cu1 O3B	2.645(5)	O2A Cu1 O4C	88.4(2)
Cu1 O3C	1.983(5)	O3A Cu1 O3B	81.15(17)
Cu1 O4C	2.338(5)	O3A Cu1 O3C	89.6(2)
Cu2 O3A	1.977(5)	O3A Cu1 O4C	97.25(19)
Cu2 O4A	2.320(5)	N2A Cu1 O2A	82.0(3)
Cu2 O3C	2.686(5)	N2A Cu1 O3A	91.3(2)
Cu2 O2D	1.930(5)	N2A Cu1 O3B	100.7(2)
Cu2 O3D	1.960(5)	N2A Cu1 O3C	171.4(2)
Cu2 N2D	1.912(6)	N2A Cu1 O4C	114.2(2)
Cu3 O3A	2.667(5)	O3C Cu1 O3B	70.93(17)
Cu3 O2B	1.951(5)	O3C Cu1 O4C	74.17(18)
Cu3 O3B	1.971(5)	O4C Cu1 O3B	145.07(17)
Cu3 N1B	1.903(6)	O3A Cu2 O4A	74.88(19)
Cu3 O3D	1.976(5)	O3A Cu2 O3C	71.31(18)
Cu3 O4D	2.325(5)	O4A Cu2 O3C	146.19(17)
Cu4 O3B	1.955(5)	O2D Cu2 O3A	95.8(2)
Cu4 O4B	2.310(5)	O2D Cu2 O4A	88.9(2)
Cu4 O2C	1.923(5)	O2D Cu2 O3C	94.75(19)
Cu4 O3C	1.946(5)	O2D Cu2 O3D	171.2(2)

Cu4 N2C	1.906(6)	O3D Cu2 O3A	90.8(2)
Cu4 O3D	2.696(5)	O3D Cu2 O4A	98.50(19)
O1A H1A	0.91(3)	O3D Cu2 O3C	81.82(18)
O1A C1A	1.340(12)	N2D Cu2 O3A	177.0(2)
O2A C7A	1.285(10)	N2D Cu2 O4A	107.1(2)
O3A C10A	1.354(8)	N2D Cu2 O3C	106.7(2)
O4A C11A	1.369(9)	N2D Cu2 O2D	82.1(2)
O4A C15A	1.428(9)	N2D Cu2 O3D	91.0(2)
N1A N2A	1.388(9)	O2B Cu3 O3A	96.28(18)
N1A C7A	1.313(10)	O2B Cu3 O3B	172.8(2)
N2A C8A	1.278(10)	O2B Cu3 O3D	95.1(2)
C1A C2A	1.388(13)	O2B Cu3 O4D	88.2(2)
C1A C6A	1.412(13)	O3B Cu3 O3A	80.39(18)
C2A C3A	1.349(16)	O3B Cu3 O3D	90.0(2)
C3A C4A	1.382(16)	O3B Cu3 O4D	98.1(2)
C4A C5A	1.392(14)	N1B Cu3 O3A	100.9(2)
C5A C6A	1.367(13)	N1B Cu3 O2B	82.2(2)
C6A C7A	1.475(12)	N1B Cu3 O3B	92.1(2)
C8A C9A	1.422(11)	N1B Cu3 O3D	172.7(2)
C9A C10A	1.389(10)	N1B Cu3 O4D	111.7(2)
C9A C14A	1.424(10)	O3D Cu3 O3A	72.59(17)
C10A C11A	1.399(11)	O3D Cu3 O4D	74.88(19)
C11A C12A	1.383(11)	O4D Cu3 O3A	147.43(16)
C12A C13A	1.382(12)	O3B Cu4 O4B	75.45(19)
C13A C14A	1.354(12)	O3B Cu4 O3D	71.77(17)
C15A C16A	1.510(14)	O4B Cu4 O3D	147.15(16)
O1B H1B	0.92(3)	O2C Cu4 O3D	93.79(19)
O1B C1B	1.331(10)	O3C Cu4 O3B	89.2(2)
O2B C7B	1.278(9)	O3C Cu4 O4B	100.0(2)
O3B C10B	1.349(9)	O3C Cu4 O3D	81.82(18)
O4B C11B	1.391(11)	N2C Cu4 O3B	172.9(2)
O4B C15B	1.443(9)	N2C Cu4 O4B	111.1(2)
N1B N2B	1.391(8)	N2C Cu4 O2C	82.6(2)
N1B C8B	1.283(9)	N2C Cu4 O3C	92.1(2)
N2B C7B	1.314(10)	N2C Cu4 O3D	101.5(2)
C1B C2B	1.382(11)	C1A O1A H1A	102(8)
C1B C6B	1.391(10)	C7A O2A Cu1	110.3(5)
C2B C3B	1.377(12)	Cu1 O3A Cu2	111.1(2)
C3B C4B	1.389(11)	Cu1 O3A Cu3	98.43(18)
C4B C5B	1.374(11)	Cu2 O3A Cu3	86.05(17)
C5B C6B	1.394(11)	C10A O3A Cu1	126.3(5)
C6B C7B	1.486(10)	C10A O3A Cu2	120.6(5)
C8B C9B	1.432(10)	C10A O3A Cu3	98.2(4)
C9B C10B	1.400(10)	C11A O4A Cu2	110.3(4)
C9B C14B	1.408(11)	C11A O4A C15A	119.0(6)
C10B C11B	1.406(10)	C15A O4A Cu2	128.7(5)
C11B C13B	1.382(11)	C7A N1A N2A	110.6(6)
C12B C13B	1.394(11)	N1A N2A Cu1	113.6(5)

C12B C14B	1.353(11)	C8A N2A Cu1	129.1(6)
C15B C16B	1.499(12)	C8A N2A N1A	117.2(7)
O1C H1C	0.90(3)	O1A C1A C2A	117.5(10)
O1C C1C	1.347(10)	O1A C1A C6A	124.1(8)
O2C C7C	1.282(9)	C2A C1A C6A	118.4(10)
O3C C10C	1.358(9)	C3A C2A C1A	121.5(11)
O4C C11C	1.371(9)	C2A C3A C4A	120.6(10)
O4C C15C	1.429(9)	C3A C4A C5A	119.2(11)
N1C N2C	1.388(8)	C6A C5A C4A	120.8(11)
N1C C7C	1.322(9)	C1A C6A C7A	121.6(9)
N2C C8C	1.266(9)	C5A C6A C1A	119.6(9)
C1C C2C	1.373(11)	C5A C6A C7A	118.7(9)
C1C C6C	1.400(11)	O2A C7A N1A	123.5(7)
C2C C3C	1.364(12)	O2A C7A C6A	120.5(8)
C3C C4C	1.370(12)	N1A C7A C6A	116.0(8)
C4C C5C	1.354(11)	N2A C8A C9A	124.2(7)
C5C C6C	1.382(11)	C8A C9A C14A	115.9(7)
C6C C7C	1.485(10)	C10A C9A C8A	125.1(7)
C8C C9C	1.445(10)	C10A C9A C14A	118.9(7)
C9C C10C	1.414(11)	O3A C10A C9A	122.3(7)
C9C C14C	1.405(10)	O3A C10A C11A	118.8(7)
C10C C11C	1.391(11)	C9A C10A C11A	118.8(7)
C11C C12C	1.358(11)	O4A C11A C10A	114.8(6)
C12C C13C	1.390(12)	O4A C11A C12A	124.2(7)
C13C C14C	1.353(11)	C12A C11A C10A	121.0(7)
C15C C16C	1.483(13)	C13A C12A C11A	120.1(8)
O1D H1D	0.90(3)	C14A C13A C12A	120.0(8)
O1D C1D	1.345(11)	C13A C14A C9A	121.1(8)
O2D C7D	1.274(9)	O4A C15A C16A	111.1(8)
O3D C10D	1.342(9)	C1B O1B H1B	95(7)
O4D C11D	1.375(9)	C7B O2B Cu3	108.9(5)
O4D C15D	1.446(9)	Cu3 O3B Cu1	98.9(2)
N1D N2D	1.410(9)	Cu4 O3B Cu1	87.87(17)
N1D C7D	1.311(10)	Cu4 O3B Cu3	110.7(2)
N2D C8D	1.281(10)	C10B O3B Cu1	100.5(4)
C1D C2D	1.403(12)	C10B O3B Cu3	125.4(4)
C1D C6D	1.406(11)	C10B O3B Cu4	120.5(4)
C2D C3D	1.353(13)	C11B O4B Cu4	109.8(4)
C3D C4D	1.382(12)	C11B O4B C15B	116.4(6)
C4D C5D	1.388(11)	C15B O4B Cu4	132.8(5)
C5D C6D	1.372(11)	N2B N1B Cu3	113.9(5)
C6D C7D	1.475(10)	C8B N1B Cu3	128.3(5)
C8D C9D	1.443(11)	C8B N1B N2B	117.7(6)
C9D C10D	1.386(11)	C7B N2B N1B	109.8(6)
C9D C14D	1.411(11)	O1B C1B C2B	116.8(7)
C10D C11D	1.402(11)	O1B C1B C6B	122.2(7)
C11D C12D	1.377(11)	C2B C1B C6B	120.9(8)
C12D C13D	1.400(12)	C3B C2B C1B	119.6(7)

C13D C14D	1.345(12)	C2B C3B C4B	120.4(8)
C15D C16D	1.488(13)	C5B C4B C3B	119.7(8)
		C4B C5B C6B	120.9(7)
		C1B C6B C5B	118.5(7)
		C1B C6B C7B	122.6(7)
		C5B C6B C7B	118.8(7)
		O2B C7B N2B	125.1(7)
		O2B C7B C6B	118.4(7)
		N2B C7B C6B	116.5(7)
		N1B C8B C9B	124.8(7)
		C10B C9B C8B	124.5(7)
		C10B C9B C14B	119.2(7)
		C14B C9B C8B	116.2(7)
		O3B C10B C9B	122.6(7)
		O3B C10B C11B	118.6(6)
		C9B C10B C11B	118.7(7)
		O4B C11B C10B	114.7(6)
		O4B C11B C13B	124.5(7)
		C13B C11B C10B	120.7(7)
		C14B C12B C13B	120.3(8)
		C11B C13B C12B	119.8(8)
		C12B C14B C9B	121.2(7)
		O4B C15B C16B	107.6(7)
		C1C O1C H1C	108(6)
		C7C O2C Cu4	109.4(4)
		Cu1 O3C Cu2	86.70(17)
		Cu4 O3C Cu1	110.6(2)
		Cu4 O3C Cu2	98.1(2)
		C10C O3C Cu1	119.5(4)
		C10C O3C Cu2	104.0(4)
		C10C O3C Cu4	125.8(4)
		C11C O4C Cu1	110.0(4)
		C11C O4C C15C	115.8(6)
		C15C O4C Cu1	134.2(5)
		C7C N1C N2C	109.5(6)
		N1C N2C Cu4	113.6(4)
		C8C N2C Cu4	128.2(5)
		C8C N2C N1C	117.8(6)
		O1C C1C C2C	119.4(8)
		O1C C1C C6C	121.7(7)
		C2C C1C C6C	119.0(8)
		C3C C2C C1C	120.1(8)
		C2C C3C C4C	121.4(8)
		C5C C4C C3C	118.5(8)
		C4C C5C C6C	122.0(8)
		C1C C6C C7C	121.8(7)
		C5C C6C C1C	118.4(7)
		C5C C6C C7C	119.5(7)

	O2C C7C N1C	124.7(7)
	O2C C7C C6C	118.6(6)
	N1C C7C C6C	116.6(7)
	N2C C8C C9C	124.7(7)
	C10C C9C C8C	123.9(7)
	C14C C9C C8C	117.0(7)
	C14C C9C C10C	119.0(7)
	O3C C10C C9C	122.2(6)
	O3C C10C C11C	119.7(7)
	C11C C10C C9C	118.1(7)
	O4C C11C C10C	113.9(6)
	C12C C11C O4C	124.2(7)
	C12C C11C C10C	121.8(7)
	C11C C12C C13C	115.9(7)
	C14C C13C C12C	119.9(8)
	C13C C14C C9C	120.8(7)
	O4C C15C C16C	106.5(7)
	C1D O1D H1D	112(8)
	C7D O2D Cu2	110.3(5)
	Cu2 O3D Cu3	109.2(2)
	Cu2 O3D Cu4	97.37(19)
	Cu3 O3D Cu4	86.05(18)
	C10D O3D Cu2	126.6(4)
	C10D O3D Cu3	119.7(4)
	C10D O3D Cu4	105.7(4)
	C11D O4D Cu3	108.8(4)
	C11D O4D C15D	117.6(6)
	C15D O4D Cu3	133.6(5)
	C7D N1D N2D	109.5(6)
	N1D N2D Cu2	113.3(5)
	C8D N2D Cu2	129.2(5)
	C8D N2D N1D	117.4(6)
	O1D C1D C2D	117.3(8)
	O1D C1D C6D	123.4(7)
	C2D C1D C6D	119.2(9)
	C3D C2D C1D	120.8(9)
	C2D C3D C4D	120.9(8)
	C3D C4D C5D	118.5(9)
	C6D C5D C4D	122.4(8)
	C1D C6D C7D	122.3(8)
	C5D C6D C1D	118.2(7)
	C5D C6D C7D	119.4(7)
	O2D C7D N1D	124.7(7)
	O2D C7D C6D	118.8(7)
	N1D C7D C6D	116.5(7)
	N2D C8D C9D	123.8(7)
	C10D C9D C8D	124.4(7)
	C10D C9D C14D	119.7(8)

	C14D C9D C8D	115.8(7)
	O3D C10D C9D	123.0(7)
	O3D C10D C11D	118.6(7)
	C9D C10D C11D	118.3(7)
	O4D C11D C10D	115.1(7)
	O4D C11D C12D	123.8(7)
	C12D C11D C10D	121.1(7)
	C11D C12D C13D	119.8(8)
	C14D C13D C12D	119.7(8)
	C13D C14D C9D	121.3(8)
	O4D C15D C16D	106.7(7)

Table S3 Comparison of the present probe with pioneering OCl⁻ probes

Sl. No	Media	Sensing mode	Mechanism	LOD	Reference
1	Aqueous medium (0.1M phosphate buffer, pH 8.5)	Turn on	Spirolactam ring opening	0.024 μM	<i>Anal. Chim. Acta</i> , 2013, 775 , 100–105
2	DMSO/H ₂ O (7/3, v/v)	Turn on	Oxidation of imine bond	0.136 μM	<i>Dyes Pigm.</i> , 2020, 174 , 108019
3	PBS buffer (10 mM, pH = 7.4).	Turn on	ESIPT	8.9 nM	<i>Sens. Actuators, B</i> , 2017, 243 , 22–28
4	PBS buffer (pH 7.2 –7.4, 10 mM, 20% EtOH)	Turn on	Oxidation triggered inhibition of ICT	6.82 nM	<i>Dyes Pigm.</i> , 2020, 182 , 108675
5	DMF	Turn on	Oxidation of imine bond	4.2 μM	<i>Spectrochim. Acta, Part A</i> , 2021, 261 , 120059
6	CH ₃ OH-water (1:9 v/v)	Turn On	AIE	0.3515 μM	<i>J. Hazard. Mater.</i> , 2021, 418 , 126243
7	Aqueous medium (10 mM HEPES buffer, pH, 7.4)	Turn On	Oxidative hydrolysis of hydrazide	59 nM	<i>Sens. Actuators, B</i> , 2018, 255 , 1112–1118
8	MeCN–PBS (3 : 7, v/v, pH, 7.4)	Turn On	Spirolactam ring opening	1.06×10 ⁻⁹ M	<i>RSC Adv.</i> , 2015, 5 , 99664–99668
9	CH ₃ CN–H ₂ O (4: 6, v/v)	Turn On	Disruption of ICT by breaking the donor-acceptor connection	1.07 μM	<i>Dalton Trans.</i> , 2013, 42 , 10097–10101
10	EtOH: H ₂ O = 1:1 (v/v)	Turn On	Oxidative splitting of the recognition group	80 nM	<i>Anal. Chim. Acta</i> , 2019, 1078 , 135–141
11	EtOH/ H ₂ O (1/1, v/v, pH 7.4)	Turn On	Reticence of ESIPT	13.87 nM	Present work

Table S4 Fluorescence life time data of C1 and C1-OCl⁻ adduct

sample	B ₁	B ₂	t ₁ (ns)	t ₂ (ns)	χ ²
C1	59.36	40.64	0.1	0.6	1.22
C1-OCl ⁻	20.41	79.59	1.38	0.63	1.16